Quantum Monte Carlo study of the H^- impurity in small helium clusters

Mose' Casalegno,[a] Massimo Mella,[b] and Gabriele Morosi[c]
Dipartimento di Chimica Fisica ed Elettrochimica, Universita' degli Studi di Milano, via Golgi 19, 20133 Milano, Italy

Dario Bressanini[d]
Dipartimento di Scienze Chimiche, Fisiche e Matematiche, Universita' dell'Insubria, Polo di Como, via Lucini 3, 22100 Como, Italy

(Received 12 May 1999; accepted 5 October 1999)

We report ground state energies and structural properties for small helium clusters (^{4}He) containing a H^- impurity computed by means of variational and diffusion Monte Carlo methods. Except for $^4He_2H^-$ that has a noticeable contribution from collinear geometries where the H^- impurity lies between the two ^{4}He atoms, our results show that $^4He_NH^-$ clusters have a compact ^4He_N subsystem that binds the H^- impurity on its surface. The results for $N \geqslant 3$ can be interpreted invoking the different features of the minima of the He–He and He–H^- interaction potentials. © *2000 American Institute of Physics.* [S0021-9606(00)50501-7]

I. INTRODUCTION

Weakly bound atomic and molecular clusters represent an interesting and growing field of research in both chemistry and physics.[1] They are useful to understand the evolution of the properties from microscopic systems to bulk matter. Moreover, they generate alluring questions whose answers are not trivial due to the important interplay between dynamical and geometrical factors in the cluster description.[1,2] Among the most studied systems, rare gas clusters possess a rich and intriguing set of properties directly related to the weakness of the interaction between their constituent atoms.[1] The shallow well of their interaction potential energy surface (PES) allows the rare gas atoms in a cluster to have large amplitude vibrational motions, therefore sampling all the features of the PES itself, and precluding the use of the usual harmonic approximation to describe their vibrational energy levels.[3]

Moreover, the clusters of the lightest rare gases undergo a solid–liquid transition at temperatures of the order of few Kelvins, so they represent good candidates as a medium where reactions can take place, allowing to study and develop low temperature chemistry. Unfortunately, a direct spectroscopic study of the droplets of rare gases to acquire accurate information about their internal dynamics is not easy to carry out, due to the absence of any chromophoric unit.[1] Furthermore, molecular beam experiments generate a too low concentration of small clusters to allow neutron scattering studies of the internal structure.[1]

Recently, after the discovery that rare gas clusters can easily pick up one or more atomic and molecular impurities,[4] attention has been paid to study the effect of the impurity on the cluster and vice versa.[5–14] These studies focused especially on the spectroscopic properties of the impurity in the cluster medium, as a tool to probe the dynamics of the cluster itself. The necessity to supplement the experimental spectroscopic results with an interpretation of the measured properties has recently renewed the theoretical interest on these species. Among the most frequent computational studies[8,10,12,14] there are the test of the accuracy of the available PES describing the interaction between the various atoms and molecules, and the calculation of the effect on the measured spectroscopic quantities of the increase of the dimension of the cluster (i.e., the number of rare gas atoms).

Among the rare gas atoms, ^{4}He owes its importance to the strong quantum features it displays in clusters and in liquid bulk at low temperatures.[1] These features are responsible for the macroscopic superfluid behavior of ^{4}He, that manifests itself in the total absence of viscosity and in the ability to quickly transport the heat from a source to the surrounding matter.[15,16]

Differently from ^{4}He, heavier rare gases show a more ''classical'' behavior; although their motions are still highly anharmonic, they present average interatomic distributions resembling the minimum energy geometry distributions. This difference can be attributed both to the heavier masses of the rare gas and to the stronger interaction between the atoms.[10–12,14]

In the remaining of this article we concentrate on the characteristic features of the doped ^{4}He clusters, which are far more interesting and complicated than the heavier rare gas ones.

A recent experiment on the OCS molecule absorbed in small ^{4}He clusters has definitively shown that superfluidity can be found even in microscopic aggregates, putting an end to a long debate.[17] Moreover, the low temperature of these clusters can help spectroscopic studies on large molecules; the electronic spectra of the amino acids tryptophan and tyrosine were simplified by cooling their vibrational motion inside an ^{4}He droplet,[18] allowing an easier interpretation of the experimental results.

While alkali and alkali-earth atoms are adsorbed on ^{4}He

[a]Electronic mail: Mose.Casalegno@unimi.it
[b]Electronic mail: Massimo.Mella@unimi.it
[c]Electronic mail: Gabriele.Morosi@unimi.it
[d]Electronic mail: dario@fis.unico.it

clusters and then investigated by electronic spectra,[19,20] all other impurities, studied by means of infrared spectroscopy, reside inside the clusters themselves,[6,17] and strongly perturbate their structure and properties. This difference is due to the weaker or stronger interactions between the helium atom and the doping molecule than between two helium atoms. Different information on the total dynamics of these aggregates could be extracted if the impurity perturbates only slightly the cluster, or even if, when attached to the droplet, it generates a system whose global properties can be studied by means of microwave or infrared techniques.

Recently, a high accuracy PES for the helium–hydride ion interaction has become available;[21] the main features of this interaction potential are the small depth (about 4 cm^{-1}), and the large value of the distance where the minimum is located (about 13 bohr). These features show themselves in the wide amplitude motion of the dimer (the mean value for the $^4He–H^-$ distance is about 22 bohr), and in the long tail of the vibrational ground state wave function. An interesting property of this quantum system is given by the existence of an excited rotational state with $J=1$.[21] A recent calculation by Li and Lin[22] using a model potential provided and indipendent check of these results, even if no quantitative agreement could be expected.

The weak interaction between He and H^- makes the hydride anion a good candidate for studies on the He clusters weakly perturbed by an impurity. Due to the presence of a negative charge that is able to polarize the helium atom, the HeH^- system should have a finite dipole moment, hence to be microwave active. Moreover, because of the small mass difference between ^4He and H^-, the spectroscopic techniques should probe the quantum motion of the whole system. This could be the case also for clusters containing more helium atoms, allowing, as stated before, to collect different information about the quantum dynamics of these aggregates.

In this article we studied both the energetics and structures of the ground state of the $^4He_NH^-$ clusters using quantum Monte Carlo (QMC) methods. During the last few years, these methods have been proved to give quite accurate information even for highly quantum systems like helium clusters.[23–25] The main goal of this study is to obtain a clear picture of the relative motion and distribution between the ^4He and the H^- species, with a special emphasis on the location of the H^- impurity with respect to the ^4He_N moiety.

The remainder of the paper is organized as follows: Sec. II contains the description of the theoretical approach, of the interaction potentials used and few comments about the Monte Carlo simulations. Section III contains the discussion of the Monte Carlo results, while Sec. IV reports our conclusions and possible future directions of this study.

II. METHODS

In atomic units, the Hamiltonian operator for any $^4He_NH^-$ clusters containing N ^4He atoms and one H^- ion is

$$\mathcal{H}=-\frac{1}{2}\left(\sum_{i=1}^{N}\frac{\nabla_i^2}{m_{^4\mathrm{He}}}+\frac{\nabla_{\mathrm{H}^-}^2}{m_{\mathrm{H}^-}}\right)+V(\mathbf{R}), \tag{1}$$

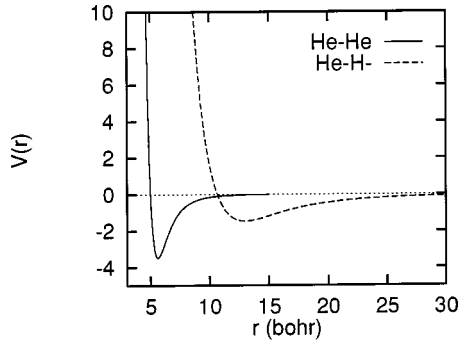

FIG. 1. He–He and He–H^- interaction potentials (μhartree).

where $V(\mathbf{R})$ is the interaction potential and $\mathbf{R}$ is a point in configuration space. Here, we assume a pair potential of the form

$$V(\mathbf{R})=\sum_{i<j}V_{\mathrm{HeHe}}(r_{ij})+\sum_{i}V_{\mathrm{HeH}^-}(r_i), \tag{2}$$

where r_{ij} is the distance between the ith and jth helium atom, while r_i is the distance between the ith helium atom and the hydride ion. In this work, for $V_{\mathrm{HeHe}}(r_{ij})$ we employ the recent Tang–Toennies–Yiu (TTY) pair potential[26] that is not based on any kind of empirical information. This choice allows us to directly compare our results with the recent ones obtained by Lewerenz,[25] who used this pair potential to compute energetics and structure of various small ^4He_N clusters. To obtain the pair potential between He and H^- we fitted the accurate full configuration interaction results by Bendazzoli, Evangelisti, and Passarini[21] employing an analytical form tailored to approximate all the three regions of the potential energy curve with similar accuracy,

$$V_{\mathrm{HeH}^-}(r)=a_1r^{a_2}e^{-a_3r}+a_4 \quad r<10\,\mathrm{bohr}, \tag{3}$$

$$V_{\mathrm{HeH}^-}(r)=a_5(1-e^{-a_6(r-a_7)})^2-a_8 \quad 10\,\mathrm{bohr}\leqslant r\leqslant 20\,\mathrm{bohr}, \tag{4}$$

$$V_{\mathrm{HeH}^-}(r)=-\frac{a_9}{r^4} \quad r>20\,\mathrm{bohr}. \tag{5}$$

This approach differs from the one used by Bendazzoli, Evangelisti, and Passarini in their work, since they chose to interpolate their data using exponential splines instead of fitting them with any analytical model. To fit the 19 computed values of the interaction potential with our analytical model, we used the Levenberg–Marquard algorithm, imposing analytically the continuity between the functions at 10 and 20 bohr. The parameters obtained by means of this procedure are (in atomic units): $a_1=1.303\,648$, $a_2=-1.297\,418$, $a_3=0.750\,314\,6$, $a_4=-0.000\,019\,89$, $a_5=0.000\,012\,769$, $a_6=0.313\,155$, $a_7=13.0$, $a_8=0.000\,014\,67$, and $a_9=0.736\,841$. Figure 1 shows both the fitted $V_{\mathrm{HeH}^-}(r)$ and the TTY $V_{\mathrm{HeHe}}(r)$ potentials. From Fig. 1, one can note that the two potentials have quite different well depth and location of the minimum; these results can be explained remembering that H^- is very diffuse, and for this reason the repulsive interaction starts at large internuclear separation. Therefore, the attractive charge-induced dipole interaction should be very weak and the well depth quite small. For the chosen

form of the model potential we used, our a_9 parameter should represent the C_4 coefficient of the standard charge-induced dipole interaction. This value was already computed by Spelsberg, Lorenz, and Meyer[27] to be 0.694 by means of sophisticated atomic calculations. Although our a_9 value differs from their by less than 5%, some doubt might arise about the accuracy of our fitted potential. Since in the $20 \leqslant r < \infty$ region the fitting of the *ab initio* computed potential by our model appears quite accurate, this difference should be due to different accuracy of the *ab initio* results by Bendazzoli, Evangelisti, and Passarini with respect to the ones obtained by Spelsberg, Lorenz, and Meyer.[27] Comparing the results computed with various methods and basis sets in Ref. 21, one could get a feeling about their relative accuracy. From this comparison we do not expect the full configuration interaction results to be more accurate than 5% of their value for all the range of distances studied. This might explain the difference between our a_9 and the C_4 by Spelsberg, Lorenz, and Meyer.

Employing our model potential, we solved the Schrödinger equation for the He–H^- system using the grid method proposed by Tobin and Hinze[28] obtaining $-0.3980\ \mathrm{cm}^{-1}$ as ground state energy. This value is in fair agreement with the result of $-0.4000\ \mathrm{cm}^{-1}$ obtained by Bendazzoli, Evangelisti, and Passarini.[21]

In this work we do not introduce any kind of information about three-body forces. For pure helium clusters one could use the standard Axilrod–Teller term[29] to augment the pair potential approximation. As to $^4He_2H^-$ three-body contribution to the potential energy an estimation can be easily given using simple electrostatic concepts. Employing the formulas for the dipole–dipole interaction energy and for the charge-induced dipole presented in Ref. 30 one obtains that the charge-induced dipole-induced dipole interaction E_{cdd} for an isosceles triangle configuration is given by

$$E_{cdd} = -\frac{\alpha^2 Z^2}{R^3 r^4}[1 - 3\cos^3(\theta)], \tag{6}$$

where α is the dipole polarizability of He, R is the distance between the two He atoms, r is the distance between He and H^-, Z is the ion charge, and θ is the angle between the He–He and He–H^- vectors. For R and r equal to the equilibrium distances of the He–He and He–H^- potentials, this term is of the order of 10^{-7}hartree, i.e., two orders of magnitude smaller than the depth of the He–H^- potential well. Moreover, recent calculations carried out on the $^4He_2H^-$ trimer by Bendazzoli[31] show no appearance of three-body effects in the potential energy surface.

To approximate the ground state wave functions for these systems, we employed the commonly used pair product form,[24]

$$\Psi_T(\mathbf{R}) = \prod_{i<j}^{N} \psi(r_{ij}) \prod_{i}^{N} \phi(r_i) \tag{7}$$

and no one-body part was used. This fact guarantees that we do not introduce any center-of-mass kinetic energy component in the description of the cluster, avoiding us the burden of subtracting it to obtain the internal energy of the system. Both the $\psi(r)$ and $\phi(r)$ functions have the same analytical form,

$$\psi(r) = \phi(r) = \exp\left[-\frac{p_5}{r^5} - \frac{p_3}{r^3} - \frac{p_2}{r^2} - p_1 r - p_0 \ln(r) \right]. \tag{8}$$

This form is identical to the one employed by Rick, Lynch, and Doll[24] except for the presence of the new term $-p_3/r^3$ previously used by Barnett and Whaley[23] in their study of helium clusters. During the preliminary stages of our work, this term was found to improve significantly the variational energy of the wave function, and to have a positive impact on the stability of the wave function optimization.

The chosen form for the trial wave function makes impossible to compute analytically the matrix elements of the Hamiltonian operator, and numerical methods must be used to obtain the energy and other mean values for a given trial wave function. The variational Monte Carlo (VMC) method is well suited for this goal since it requires only the evaluation of the trial wave function, its gradient, and its Laplacian. Since this and other Monte Carlo methods are well described in the literature,[32] we refer the reader to it and to our previous work in this field for the details. However, it is relevant to point out that all the mean values were computed by means of the general integral,

$$\langle \mathcal{O} \rangle = \frac{\int f(\mathbf{R}) \mathcal{O}_{\mathrm{loc}}(\mathbf{R}) d\mathbf{R}}{\int f(\mathbf{R}) d\mathbf{R}}, \tag{9}$$

where

$$\mathcal{O}_{\mathrm{loc}}(\mathbf{R}) = \frac{\mathcal{O}\Psi_T(\mathbf{R})}{\Psi_T(\mathbf{R})} \tag{10}$$

and $f(\mathbf{R}) = \Psi_T^2(\mathbf{R})$ for VMC, while $f(\mathbf{R}) = \Psi_T(\mathbf{R})\Psi_0(\mathbf{R})$ for diffusion Monte Carlo (DMC). In VMC calculations, Eq. (9) gives the expectation value of the $\mathcal{O}$ operator over the trial wave function Ψ_T, while in DMC simulations Eq. (9) gives an improved estimate of the value, or the exact result if the $\mathcal{O}$ operator does not commute or commutes with the Hamiltonian.

As to our general strategy to optimize the trial wave functions for the clusters studied, we usually select the parameters of the exponential part in Eq. (8) by minimizing the estimate of the variance of the local energy over a fixed sample of walkers,

$$\sigma^2 = \frac{1}{N_{\mathrm{walker}}} \sum_{i=1}^{N_{\mathrm{walker}}} [E_{\mathrm{loc}}(\mathbf{R}_i) - E_{\mathrm{ref}}]^2. \tag{11}$$

All the VMC optimization, and the VMC and DMC simulations were carried out using at least 5000 walkers; all the DMC simulations were run employing a time step of 200 $\mathrm{hartree}^{-1}$ and the accuracy of the results was checked running few more simulations with smaller time steps to ensure that the time step bias was negligible for all the expectation values.

The wave function parameters are presented in Table I for all the clusters studied in this work.

TABLE I. Parameters of the optimized trial wave functions.

N_{He}	$\phi\, p_5$	p_3	p_2	p_1	p_0	$\psi\, p_5$	p_2	p_1	p_0
1	6725.6	1922.3	12.44	0.0863	0.342				
2	0.0	1531.0	41.89	0.0707	0.429	2654.5	12.26	0.0594	0.817
3	27.7	1531.6	9.40	0.0616	0.242	2854.5	10.33	0.0564	0.616
4	154.5	1317.6	10.60	0.0571	0.126	2323.9	18.23	0.0654	0.548
5	381.0	1015.2	51.37	0.0476	0.353	2410.2	22.60	0.0	1.151
6	1588.1	978.3	45.62	0.0457	0.255	2339.5	22.96	0.0028	1.122
7	6293.5	986.6	34.62	0.0462	0.139	2304.0	21.96	0.0105	0.885
8	10791.7	946.8	11.40	0.0369	0.222	2165.2	26.39	0.0083	0.944
9	5466.4	944.5	23.71	0.0420	0.101	2474.2	18.97	0.0034	0.880
10	5221.4	836.9	10.10	0.0352	0.0	2328.0	19.49	0.0044	0.798
11	5221.4	836.9	10.10	0.0352	0.0	2328.0	19.49	0.0044	0.798
12	5221.4	836.9	10.10	0.0352	0.0	2328.0	19.49	0.0044	0.798

III. RESULTS AND DISCUSSION

In order to check our code, we carried out DMC simulations on the small systems $^4He_2$, $^4He_3$, and $^4He_4$ employing the parameter listed in Ref. 24 for the trial wave functions. Our DMC results, $-0.000\,89(1)$ cm^{-1} for $^4He_2$, $-0.087\,84(7)$ cm^{-1} for $^4He_3$ and $-0.3886(1)$ cm^{-1} for $^4He_4$, are in optimal agreement with the results obtained by Lewerenz.[25] As far as $^4HeH^-$ is concerned, we optimized a wave function of the form of Eq. (8) obtaining $-0.369\,87(8)$ cm^{-1} as mean energy. Using this trial wave function we obtained a DMC energy of $-0.3969(4)$ cm^{-1}, in agreement with the result of -0.3980 cm^{-1} previously obtained by means of a grid method.

The remaining small discrepancy with the result by Bendazzoli, Evangelisti, and Passarini[21] is due to the different method we used to obtain an analytical representation of the interaction potential, and shows the accuracy of the fitted potential.

These results allow a first comparison between $^4He_2$ and $^4HeH^-$; although the well depth of the interaction potential energy between two helium atoms is almost twice the well depth of the HeH^- potential, and the reduced mass of $^4HeH^-$ is smaller than the one of $^4He_2$, the total energies differ by more than two orders of magnitude favoring the stability of $^4HeH^-$. This outcome can be explained observing that the HeH^- potential has a longer asymptotic decay and a shallower well than the He–He potential. These features reflect themselves in a narrower wave function and a smaller mean distance between ^4He and H^- than between ^4He and ^4He.

Having tested our code, we optimized a trial wave function for the smallest cluster $^4He_2H^-$ starting from the parameters of the wave functions of the two dimers $^4He_2$ and $^4HeH^-$. Since this initial wave function was a crude approximation to the ground state, instead of using a VMC distribution of walkers to carry out the parameter optimization, we employed a DMC simulation to select the configurations. This alternative way, although seldom used, has the advantage to push the distribution towards the correct one, biasing the selection of the parameters of the trial wave function toward better ones. After a couple of optimization steps using the DMC distributions, the wave function parameters had roughly converged, allowing us to use VMC simulations to compute mean values and to select the new configurations to carry out the optimization procedure itself for this small system.

For all the $^4He_NH^-$ systems with $N>2$ the wave function optimization was started using the parameters of the cluster having one helium atom less. We found this choice to be a good initial guess for the minimization procedure and to select the set of configurations by means of a VMC simulation. The VMC results obtained by means of the optimization of the trial wave function for the $^4He_NH^-$ are shown in Table II.

Since our trial wave functions are only an approximation

TABLE II. VMC and DMC energy and mean potential results for the $^4He_NH^-$ clusters. All energy values are in cm^{-1}.

N	E_0^{VMC}	V_0^{VMC}	σ	E_0^{DMC}	V_0^{DMC}	E_0^{VMC}/E_0^{DMC}
2	−1.0565(15)	−2.9628(87)	1.291(11)	−1.0912(7)	−2.9804(21)	0.97
3	−1.9673(2)	−5.7457(22)	1.927(17)	−2.0476(20)	−5.7918(65)	0.95
4	−3.0392(15)	−9.633(11)	2.458(22)	−3.2569(66)	−9.656(22)	0.94
5	−4.3718(21)	−12.424(13)	2.941(65)	−4.6725(43)	−13.280(13)	0.93
6	−5.8072(43)	−17.601(15)	3.928(44)	−6.2570(44)	−18.628(19)	0.93
7	−7.3083(21)	−22.314(13)	4.433(43)	−7.9667(65)	−23.219(22)	0.91
8	−8.8820(44)	−28.356(20)	5.421(44)	−9.799(18)	−29.211(66)	0.90
9	−10.5718(65)	−35.956(17)	7.023(65)	−11.763(22)	−35.70(13)	0.89
10	−12.2025(66)	−39.329(22)	7.638(21)	−13.850(11)	−40.73(12)	0.88
11	−13.703(11)	−48.305(44)	9.437(64)	−15.990(17)	−48.54(16)	0.85
12	−14.900(17)	−58.27(11)	11.588(65)	−18.220(15)	−57.21(22)	0.82

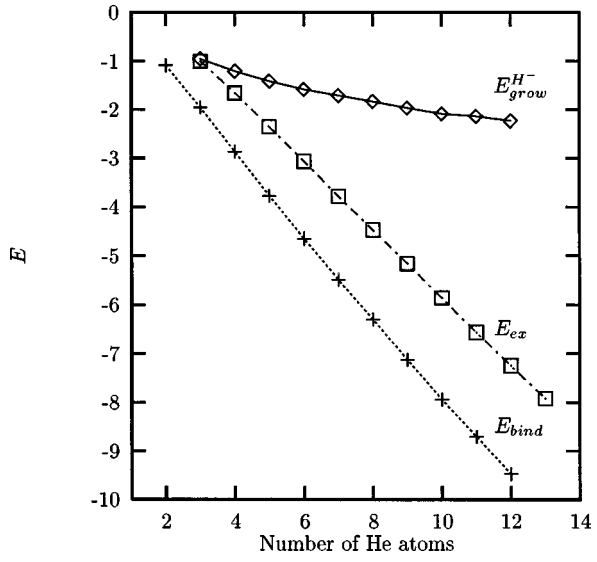

FIG. 2. E_{bind}, $E^{\text{H}^-}_{\text{grow}}$ and E_{ex} vs the number of He atoms for the $^4\text{He}_N\text{H}^-$ clusters. Energies are in cm^{-1}.

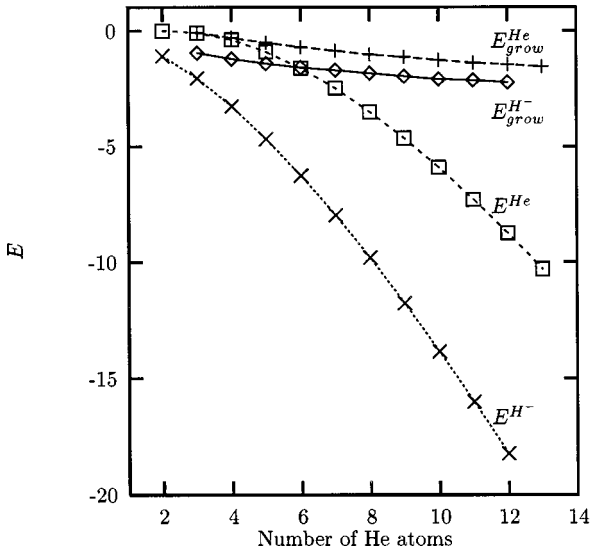

FIG. 3. Total energy and E_{grow} for both pure He and H^- doped clusters. Energies are in cm^{-1}.

of the true ground state functions and allow to compute only approximate properties of these clusters, to project out all the remaining excited state contributions we employed DMC simulations to sample the distribution $f(\mathbf{R}) = \Psi_T(\mathbf{R})\Psi_0(\mathbf{R})$. VMC and DMC energy and potential mean values are shown in Table II. Comparing DMC and VMC energy results, one can note that the percentage of total energy recovered by the VMC wave functions decreases in monotonic fashion, starting from 97% for the $N=2$ cluster and ending to 82% for the largest cluster $N=12$ studied in this work. At present, we are not able to include any definitive explanation of this behavior, but we feel that it could be due either to the limitation of the model function itself or to the optimization procedure based on the variance of the local energy, or both.

Differently from what has been noted in Ref. 25 for the pure helium clusters, energies and other mean values for the $^4\text{He}_N\text{H}^-$ systems converged quite easily even for the smallest clusters with $N \leqslant 4$.

From the results shown in Table II, supplemented with the DMC results by Lewerenz on pure helium clusters, one can compute various interesting energetic quantities:

$$
\begin{aligned}
E_{\text{ex}}(N) &= E_{^4\text{He}_N} - E_{^4\text{He}_{N-1}\text{H}^-}, \\
E^{\text{H}^-}_{\text{grow}}(N) &= E_{^4\text{He}_{N-1}\text{H}^-} - E_{^4\text{He}_N\text{H}^-}, \\
E^{\text{He}}_{\text{grow}}(N) &= E_{^4\text{He}_{N-1}} - E_{^4\text{He}_N}, \\
E_{\text{bind}}(N) &= E_{^4\text{He}_N} - E_{^4\text{He}_N\text{H}^-}, \qquad (12)
\end{aligned}
$$

where $E_{\text{ex}}(N)$ represents the energy that is released exchanging an helium atom with the hydride ion, $E^{\text{H}^-}_{\text{grow}}(N)$ and $E^{\text{He}}_{\text{grow}}(N)$ the energies that are released adding a ^4He to an already formed $^4\text{He}_{N-1}\text{H}^-$ or $^4\text{He}_{N-1}$ cluster, respectively, while $E_{\text{bind}}(N)$ is the binding energy of H^- to the $^4\text{He}_N$ cluster. These quantities are shown in Figs. 2 and 3 to allow a quick comparison, together with the total energy and $E_{\text{grow}}(N)$ for the pure helium clusters obtained by Lewerenz. We supplemented his results with the total energy for $^4\text{He}_{11}$ ($-7.288(3)$ cm^{-1}), $^4\text{He}_{12}$ ($-8.746(7)$ cm^{-1}), $^4\text{He}_{13}$ ($-10.299(4)$ cm^{-1}) computed in this study.

Similarly to the results obtained by Barnett and Whaley[5] in their work on helium clusters containing an hydrogen molecule as impurity, from Figs. 2 and 3 it is possible to note that the energetics of these small $^4\text{He}_N\text{H}^-$ clusters is dominated by the presence of the H^- ion. The total energy of the $^4\text{He}_N\text{H}^-$ appears to be much lower than the energy of $^4\text{He}_N$. For the clusters we studied, both $E_{\text{bind}}(N)$ and $E_{\text{grow}}(N)$ increase almost linearly with the number of helium atoms. This is an expected result for $E_{\text{grow}}(N)$ since, if no three-body contribution to the potential energy is present, the total energy of a cluster should be roughly proportional to the number of pairs present. As far as $E_{\text{bind}}(N)$ is concerned, its almost linear behavior cannot be explained by means of a similar reasoning; this outcome could be easily rationalized if H^- were solvated by the He atoms. Unfortunately this appears to be hardly possible, due to the quite different well minimum location of the two potentials.

To obtain information about the structure of doped clusters, during the DMC simulations we collected the radial distribution $R(r)$ from the center of mass for both ^4He and H^-,

$$
\mathbf{R}_{\text{CM}} = \frac{m_{^4\text{He}} \Sigma_{i=1}^{N} \mathbf{r}_i + m_{\text{H}^-}\mathbf{r}_{\text{H}^-}}{N_{\text{He}} m_{^4\text{He}} + m_{\text{H}^-}} \qquad (13)
$$

and from the geometrical center of the cluster

$$
\mathbf{R}_G = \frac{\Sigma_{i=1}^{N} \mathbf{r}_i + \mathbf{r}_{\text{H}^-}}{N_{\text{He}} + 1}. \qquad (14)
$$

Figures 4 and 5 display the results for $R(r)$ respect to the geometrical center; these are normalized such that

$$
\int_0^{\infty} R(r)_{\text{He}} r^2 dr = N_{\text{He}} \qquad (15)
$$

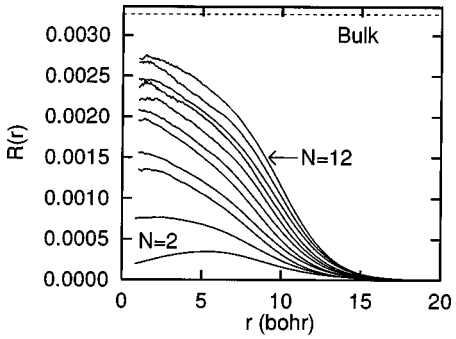

FIG. 4. Radial density distribution of the He atoms with respect to the geometrical center of the clusters.

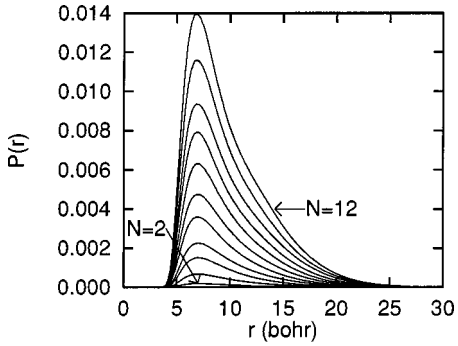

FIG. 6. He–He pair distribution in the clusters.

for the helium atoms, while

$$\int_0^\infty R(r)_{\mathrm{H}^-} r^2 dr = 1 \tag{16}$$

for the H^- ion. We chose to show only $R(r)$ with respect to the geometrical center, since the same quantity computed with respect to the center of mass does not introduce any new information.

Comparing the He radial density distributions shown in Fig. 4 with the same profiles obtained by Lewerenz,[25] it is possible to note that they appear quite similar except for our three-body cluster, i.e., $^4He_2H^-$. The He density distribution for this cluster shows a maximum around 5.30 bohr, but there is no trace of the rise of the density for small distances from the center that can be seen in the case of $^4He_3$. Nevertheless, the plot of Fig. 4 shows that He can occupy the geometrical center position, i.e., $^4He_2H^-$ in its ground state can be found in the linear geometry where the H^- ion is external to the $^4He_2$ moiety. Increasing the number of He atoms present in the cluster, the density near the cluster center rises toward the bulk value, represented in Fig. 4 by the horizontal dashed line. Similarly to the pure He clusters, the helium atoms appear to be completely delocalized with no indication of any shell filling structure.

The H^- density distributions shown in Fig. 5, show evidence of a peaked distribution of the impurity with respect to the shallower profile of the He atoms. Upon increasing the number of helium atoms in the cluster, the H^- is pushed toward larger distances from the center and the penetration of H^- decreases in a fairly monotonic fashion. The only exception to this behavior is the smallest cluster $^4He_2H^-$; its distribution shows a rise beyond statistical fluctuation for a distance from the center less than the minimum located around 4.1 bohr. This result indicates that in the $^4He_2H^-$ cluster the linear geometry where H^- lies between the He atoms plays a significant role although H^- has a larger probability to lie 10 bohr away from the center of the cluster. Concluding, except for the smallest cluster of the series, the impurity is not solvated by the ^4He atoms, having a small probability to be found near the center of the cluster. Analogous conclusions can be obtained by the density distributions computed with respect to the center of mass of the cluster.

The pair distribution functions $P(r)$ of the ^4He–^4He and ^4He–H^- distances are shown in Figs. 6 and 7, respectively. These distributions are normalized such that $\int_0^\infty P(r) r^2 dr = N_{\mathrm{He}}$. Again, the He–He distribution has many similarities with the same quantity computed in Ref. 25, showing a short range structure given by the sharp boundary hole around each He atom and a long decaying tail for large distances. Moreover, for $N \geqslant 10$, our pair distributions show a weak shoulder around 12–13 bohr; the onset of this peculiarity of the He–He pair distribution was already noted by Barnett and Whaley[23] for $^4He_{13}$ and $^4He_{14}$ and explained by means of the appearance of the second-nearest-neighbor coordination shell. This cannot be the case for our $N = 10$–12 clusters, where the icosahedral shell filling is not even completed. A similar feature seems to appear for $^4He_{10}$ in the pair distribution shown by Lewerenz in his work on pure clusters.[25] We interpret this feature as due to the presence of a light residual of an almost icosahedral structure of the clusters,

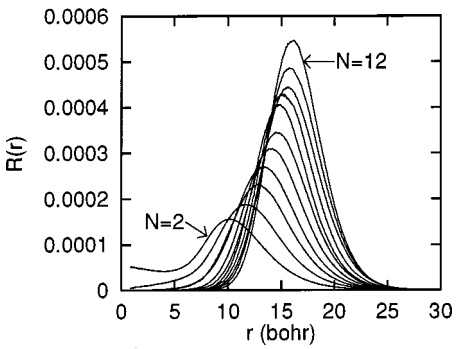

FIG. 5. Radial density distribution of the H^- ion with respect to the geometrical center of the clusters.

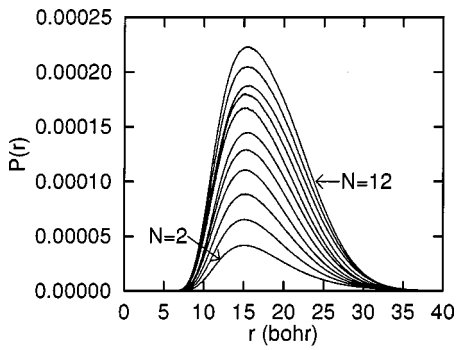

FIG. 7. He–H^- pair distribution in the clusters.

TABLE III. DMC mean values for observables of the $^4He_NH^-$ clusters. All values are in bohr.

N_{He}	$\langle r_{HeH^-}\rangle$	$\langle r_{HeHe}\rangle$	$\langle r_{H^-CM}\rangle$	$\langle r_{HeCM}\rangle$
2	21.004	14.856	12.997	9.923
3	20.380	13.234	14.153	8.941
4	20.042	12.224	14.942	8.279
5	19.964	12.210	15.251	8.263
6	20.002	12.459	15.811	8.392
7	20.172	12.621	16.221	8.567
8	20.019	12.590	16.333	8.570
9	20.257	12.798	16.717	8.674
10	20.574	12.983	17.123	8.874
11	20.547	12.920	17.236	8.889
12	20.513	12.936	17.332	8.883

i.e., ^4He does not have only first neighbors. Moreover, we suspect this trait to be emphasized by the light deformation of the ^4He_N moiety distribution due to the impurity resident on its surface. The presence of this deformation for all the studied clusters is supported by the almost linear behavior of E_{bind} shown in Fig. 2, and by the fact that only small changes take place in the form of the He–H^- distributions (Fig. 7) upon increasing of the number of atoms in the clusters.

To find a more sound support to our interpretation about the He moiety distortion for the larger studied clusters, we computed the DMC mean value $\langle\cos(\theta)\rangle$ for the angle between the vectors connecting the center of the He moiety with a He atom and the H^-. If the He moiety were spherical $\langle\cos(\theta)\rangle$ should be exactly zero by basic symmetry arguments. Any deviation from this value indicates an overall distortion of the helium subcluster. Our computed values are $\langle\cos(\theta)\rangle=-0.2084(2)$ for He_8H^-, $\langle\cos(\theta)\rangle=-0.1873(3)$ for He_9H^-, $\langle\cos(\theta)\rangle=-0.1675(2)$ for $He_{10}H^-$, $\langle\cos(\theta)\rangle=-0.1517(3)$ for $He_{11}H^-$, and $\langle\cos(\theta)\rangle=-0.1391(2)$ for $He_{12}H^-$. These results indicate a strong deformation of the He subclusters, the value of θ being on average larger than $\pi/2$. Moreover, this deformation seems to reduce on going toward larger clusters, as if the helium atom subcluster became more compact and the impurity were less able to distort the moiety.

From the sampled density and pair distributions, displayed in Figs. 4–7, various mean distances can be computed by simple one dimensional integration. In Table III, we report the values for $\langle r_{HeH^-}\rangle$, $\langle r_{HeHe}\rangle$, $\langle r_{HeCM}\rangle$, and $\langle r_{H^-CM}\rangle$. Comparing our $\langle r_{HeHe}\rangle$ and $\langle r_{HeCM}\rangle$ results with the mean values computed by Lewerenz for the clusters containing the same total number of particles, we note that our doped clusters have a more compact structure of the ^4He atom moiety than the pure ones, certainly due to the presence of the strongly binding impurity. Both mean distances show a sharp decrease up to $N=5$ where a minimum is located, and a smooth increase going towards larger N. This behavior can be explained easily by means of standard arguments; going from $N=2$ to $N=5$ the mean interaction between the particles increases due to their increased number, giving rise to a stronger binding between them. For $N>5$ the cluster becomes larger due to the addition of another ^4He atom, in spite of the augmented total interaction energy. A similar behavior is displayed by the $\langle r_{HeH^-}\rangle$ mean values, and it can be rationalized by means of the same arguments.

As far as $\langle r_{H^-CM}\rangle$ is concerned, its monotonic increase on going towards larger N can be explained, remembering that H^- stays on the surface of the He moiety, by the joined effect of the increased dimension of the ^4He atoms moiety and of the displacement of the center of mass location inside the moiety itself, due to a simple mass effect.

As previously stated, these mean values are not exact since their operators do not commute with the system Hamiltonian. To check the overall accuracy of our results, we carried out finite field calculations on the larger clusters as proposed by Sandler, Buch, and Clary[33] to obtain an independent estimation of these quantities. The difference between finite-field and mixed estimator results were found, generally, smaller than 2%–3% for all the observables, showing that our optimized trial wave functions allow accurate calculations of structural quantities for this clusters.

IV. CONCLUSIONS

In this work we presented the first quantum mechanical study of an anionic impurity in ^4He clusters. We approximated the total interaction potential as a sum of pair components, therefore excluding any non addictive effect in the description of the systems. From our semiclassical analysis of the charge-induced-dipole-induced-dipole interaction, we feel that the three-body interaction between two He and one H^- should not play a major role than in the pure He case in defining both energetics and structure of the clusters. We want to stress that the used two-body potential between He and H^-, although it represents the present state of the art for this small system, might not allow to get the finest details of the energy differences between different clusters, but that the gross picture of both energy and structure should be correctly described.

Our results show the H^- ion to be located on the surface of the cluster, except for the $^4He_2H^-$ cluster where it has a finite probability to be found between the two He atoms in a linear geometry. Our total energy values show that the interaction between helium and the impurity is an important component of the total energy of the system, while our mean geometrical values show that the helium moiety is slightly contracted with respect to the pure cluster case. We consider this fact to be due to the form of the interaction potential between an helium atom and the impurity, and especially to its longer tail respect to the He–He potential.

As far as the possibility to record a microwave spectrum of these systems is concerned, the location of the impurity on the cluster surface seems to indicate that this is possible, at least in principle. In fact, the cluster structures resemble mostly the structure of a heteronuclear diatomic molecule whose lightest atom carries a negative charge, and whose heaviest atom has a fairly large radius.

In conclusions, the effects of the isotopic substitution of H^- with D^- on the structure and energetics are worth to study, since they were found quite important for HeH^-.[21] We expect these effects to be especially important for the excited rotational states of these complexes, so we are plan-

ning to extend our study in this new direction, i.e., to compute ground state properties for clusters containing D^-, and rotational excited states for both the doping impurities.[34]

ACKNOWLEDGMENTS

This work was supported by the italian MURST Grant No. 9803246003. The authors wish to thank G. L. Bendazzoli for providing the interaction potential values between He and H^-. The authors are also indebted to the Centro CNR per lo Studio delle Relazioni tra Struttura e Reattivita' Chimica for grants of computer time. Also, this work has benefited from a postdoctoral fellowship of M.M.

[1] K. B. Whaley, Int. Rev. Phys. Chem. **13**, 41 (1994).
[2] T. González-Lezana, J. Rubayo-Soneira, S. Miret-Artéz, F. A. Gianturco, G. Delgado-Barrio, and P. Villarreal, Phys. Rev. Lett. **82**, 1648 (1999).
[3] A. Mushinski and M. P. Nightingale, J. Chem. Phys. **101**, 8831 (1994).
[4] A. Scheidemann, J. P. Tonnies, and J. A. Northby, Phys. Rev. Lett. **64**, 1899 (1990).
[5] R. N. Barnett and K. B. Whaley, J. Chem. Phys. **96**, 2953 (1992).
[6] M. A. McMahon, R. N. Barnett, and K. B. Whaley, J. Chem. Phys. **104**, 5080 (1996).
[7] S. A. Chin and E. Krotscheck, Phys. Rev. B **52**, 10405 (1995).
[8] D. Blume, M. Lewerenz, F. Huisken, and M. Kaloudis, J. Chem. Phys. **105**, 8666 (1996).
[9] M. Hartmann, N. Pörtner, B. Sarkatov, J. P. Toennies, and A. F. Vilesov, J. Chem. Phys. **110**, 5109 (1999).
[10] M. Lewerenz, J. Chem. Phys. **104**, 1028 (1996).
[11] G. de Oliveira and C. E. Dykstra, Chem. Phys. Lett. **264**, 85 (1997).
[12] T. A. Beu, Y. Okada, and K. Takeuchi, Eur. Phys. J. D **6**, 99 (1999).
[13] Y. Xu and W. Jäger, J. Chem. Phys. **107**, 4788 (1997).
[14] M. W. Severson, J. Chem. Phys. **109**, 1343 (1998).
[15] D. R. Tiley and J. Tiley, *Superfluidity and Superconductivity* (Adam Hilger, Bristol, 1986).
[16] E. B. Gordon, V. V. Khmelkenko, A. A. Pelmenev, E. A. Popov, and O. F. Pugachev, Chem. Phys. Lett. **155**, 301 (1993).
[17] S. Grebenev, J. P. Toennies, and F. Vilesov, Science **279**, 2083 (1998).
[18] A. Lindinger, J. P. Tonnies, and F. Vilesov, J. Chem. Phys. **110**, 1429 (1999).
[19] F. Stienkemeier, F. Meier, and H. O. Lutz, J. Chem. Phys. **107**, 10816 (1997).
[20] F. Stienkemeier, W. E. Ernst, J. Higgins, and G. Scoles, Phys. Rev. Lett. **74**, 3592 (1995).
[21] G. L. Bendazzoli, S. Evangelisti, and F. Passarini, Chem. Phys. **215**, 217 (1997).
[22] Yong Li and C. D. Lin, Phys. Rev. A **60**, 2009 (1999).
[23] R. N. Barnett and K. B. Whaley, Phys. Rev. A **47**, 4082 (1993).
[24] S. W. Rick, D. L. Lynch, and J. D. Doll, J. Chem. Phys. **95**, 3506 (1991).
[25] M. Lewerenz, J. Chem. Phys. **106**, 4596 (1997).
[26] K. T. Tang, J. P. Tonnies, and C. L. Yiu, Phys. Rev. Lett. **74**, 4571 (1995).
[27] D. Spelsberg, T. Lorenz, and W. Meyer, J. Chem. Phys. **99**, 7845 (1993).
[28] F. L. Tobin and J. Hinze, J. Chem. Phys. **63**, 1034 (1975).
[29] B. M. Axilrod and E. Teller, J. Chem. Phys. **11**, 299 (1943).
[30] J. Israelachvili, *Intermolecular and Surface Forces* (Academic, London, 1991).
[31] G. L. Bendazzoli (private communication).
[32] B. L. Hammond, W. A. Lester Jr., and P. J. Reynolds, *Monte Carlo Methods in Ab Initio Quantum Chemistry*, 1st ed. (World Scientific, Singapore, 1994).
[33] P. Sandler, V. Buch, and D. C. Clary, J. Chem. Phys. **101**, 6353 (1994).
[34] D. Blume, M. Mladenovic, M. Lewerenz, and K. B. Whaley, J. Chem. Phys. **110**, 5789 (1999).